Polymer Chemistry

PAPER

Check for updates

Mono- and dimeric zinc(II) complexes for PLA production and degradation into methyl lactate – a chemical recycling method†

Jack Payne,[a] Paul McKeown,[a] Mary F. Mahon,[b] Emma A. C. Emanuelsson[a,c] and Matthew D. Jones (ID) *[a,b]

A series of well-defined mono- and dimeric Zn(II)-complexes were prepared and fully characterised by X-ray crystallography and NMR spectroscopy. Their application to the ROP of *rac*-LA to produce biocompatible atactic PLA was demonstrated in both solution and under industrially preferred melt conditions at 180 °C with a [*rac*-LA] : [Init] : [BnOH] of 3000 : 1 : 10. Exceptional activity was observed in all instances, albeit with generally poor molecular weight control (M_n) and broad dispersities ($Đ$), with dimers outperforming their monomeric counterparts. The propensity of all Zn(II)-complexes to facilitate PLA degradation into methyl lactate (Me-LA) under mild conditions is also demonstrated. Zn(**2−3**)$_2$ were identified as the outstanding candidates, achieving full conversion to Me-LA within 8 h at 80 °C in THF. Further degradation kinetic analysis revealed Zn(**2−3**)$_2$ to have k_{app} values of 0.63 $\pm$ 0.051 and 0.44 $\pm$ 0.029 h^{-1} for the rate of consumption of PLA respectively.

Introduction

Petroleum-based polymers (plastics) dominate modern-day society, with annual global production exceeding 300 Mtonnes, of which *ca.* 99% were derived from petrochemical feedstocks in 2015.[1] However, it is clear polymer production based on diminishing fossil fuel reserves is unsustainable, with the oil demand for plastics anticipated to rise to 20% by 2050 from today's value of 6%.[2–5] Moreover, plastic pollution, particularly in our oceans, has reached epidemic proportions in recent years, partly due to the intrinsic robustness and durability of plastics, but primarily through the irresponsible handling of plastic waste.[6] Indeed, it is projected 250 Mtonnes of plastic waste will reside in our oceans by 2025 at current disposal rates.[4,7] There is therefore a demand for renewable and sustainable alternatives that, ideally, possess facile degradation pathways, a prerequisite to mitigating such concerns. Consequently, renewable polymers have emerged as a promising alternative to traditional polymers since they can be produced from biomass, which remains a relatively untapped, abundant resource.[3] Poly(lactic acid) (PLA), a sustainable and biocompatible aliphatic polyester, has emerged as one of the outstanding renewable alternatives within the last 20 years.[8] PLA has attracted considerable commercial and academic interest, owing to its comparable physical properties with existing synthetic plastics.[8,9] As such, PLA has found use in single-use, disposable applications in the packaging sector, but also the biomedical industry, owing to its inherent biocompatibility.[3,5,8] However, the widespread use of PLA remains limited by a high production cost, which involves the fermentation of lactic acid, prior to subsequent pre-polymerisation steps to produce the cyclic diester monomer, lactide.[9] Possible solutions include the use of shape selective catalysts and gas–phase reactions, both of which render the monomer preparation less energy and resource intensive.[10,11] However, despite its green credentials, PLA is still a possible source of plastic pollution since biodegradation occurs exclusively under industrial composting conditions.[12] Moreover, conventional waste management strategies, including landfill and incineration, align with a linear economic model, a primary contributor to the mounting plastic waste crisis. Indeed, as of 2015, *ca.* 6300 Mtonnes of plastic waste has been produced, and by 2050 it is estimated *ca.* 12 000 Mtonnes of plastic waste will reside in either landfill or the natural environment.[6] Thus, there is a clear need to develop alternative targeted waste management technologies to facilitate this transition, namely through

[a]Centre for Sustainable and Circular Technologies, University of Bath, Claverton Down, Bath, BA2 7AY, UK
[b]Department of Chemistry, University of Bath, Claverton Down, Bath, BA2 7AY, UK. E-mail: mj205@bath.ac.uk
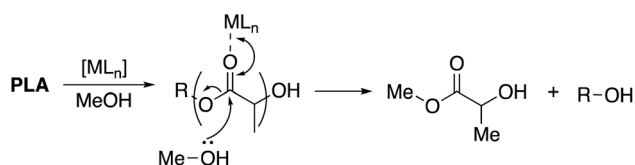[c]Department of Chemical Engineering, University of Bath, Claverton Down, Bath, BA2 7AY, UK

recycling.[4,7] Mechanical recycling is one possible solution but is limited by eventual material downgrading due to thermo-mechanical degradation, resulting in material repurposing to applications that require polymer of lower quality. A promising alternative is chemical recycling, which has the potential to reduce both waste and operational costs through material regeneration, achieved either through the depolymerisation or degradation of PLA.[13] A number of different methods have been reported in the literature, including hydrolytic and thermal degradation, as well as enzymatic processes.[14–23] However, the former two rely on high temperature conditions (200–400 °C), resulting in high operational costs, whilst uncertainty surrounds the scalability of the latter. Alternatively, the transesterification of PLA with alcohols to generate lactate esters has gathered appreciable momentum in recent years (Scheme 1). Low-molecular-weight lactate esters have been cited as green substitutes to traditional hydrocarbon-based solvents, owing to their ease of handling, low toxicity and inherent biodegradability.[24] As such, lactate esters lend themselves to a variety of different sectors, from polymer and pharmaceuticals manufacturing through to the paints and agricultural chemical industry, to name but a few.[25] Indeed, it is envisaged that this process will be viable at an industrial scale, both from an economic and environmentally sustainable perspective.[26] Furthermore, there is the potential to transform lactate esters into platform chemicals, such as lactic acid or lactide, further promoting a circular economy approach.[27–29] A number of different PLA transesterification methods have been reported in the literature.[30–44] DuPont possess a patent for PLA degradation in the presence of H_2SO_4, achieving high conversion (69–87%) to various lactate esters (R = Me, Et and ^{n}Bu) within 2 h between 150–190 °C.[30] Coszach et al.[17] demonstrated the hydrolysis of PLA to lactic acid, observing enhanced PLA dissolution and polymer separation with lactate esters as the solvent of choice. Hydrolysis proceeded both with or without NaOH, requiring elevated temperatures between 80–180 °C and pressures of up to 10 bar. Catalysts based on rare metals, including iridium and ruthenium, have also been reported for hydrogenation and hydrosilylation processes, but are unattractive options to industry due to a high metal cost.[36–38] Both Fliedel et al.[40] and McKeown et al.[41] have reported systems based on Zn(II)-complexes, with the latter achieving up to 100% Me-LA conversion within 1 h at 90 °C. Interestingly, McKeown et al.[42] recently demonstrated shifting to an analogous propylenediamine system afforded superior

activity, achieving 81% conversion within 30 minutes at 50 °C, highlighting the influence of metal–ligand relationships. Petrus et al.[43] prepared a series of lactate esters from a variety of different alcohols, reporting reaction temperatures as low as 80 °C in the presence of earth abundant metal-based catalysts, including Mg(II) and Ca(II). However, in the absence of a catalyst, reaction temperatures increased to 260 °C, thus highlighting the benefits of metal-mediated degradation, particularly from an economic and environmental standpoint. However, despite the need for simple, controlled metal-mediated degradation pathways, literature examples remain limited. There is therefore a clear opportunity to develop robust, industrially viable catalysts based on both earth abundant metals and scalable ligand systems. Herein, we report the synthesis of a series of mono- and dimeric Zn(II)-Schiff-base complexes, and their application to the ROP of rac-lactide in both solution and under industrially preferred melt conditions is demonstrated. The metal-mediated degradation of PLA into Me-LA under mild conditions is also reported, in conjunction with a reaction kinetic study.
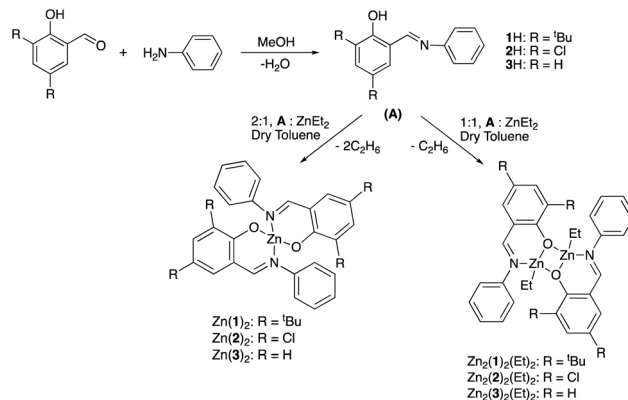
Results and discussion

Synthesis

A range of simple Schiff-base ligands were prepared via an imine condensation reaction (Scheme 2) and characterised by ^{1}H NMR spectroscopy and mass spectrometry. ^{1}H NMR singlets at ca. δ = 8 and 14 ppm were assigned to characteristic HC=N and O–H resonances respectively. Mono- and dimeric complexes of Zn(II) were then prepared in anhydrous toluene and purified by hexane recrystallisation or via washing (Scheme 2). To alleviate safety concerns associated with the pyrophoric alkyl precursor employed ($ZnEt_2$), the synthesis of $Zn(\mathbf{1})_2$ was attempted from $Zn(OAc)_2 \cdot 2H_2O$ in EtOH under reflux conditions but proved unsuccessful. In the solid state, $Zn(\mathbf{1–3})_2$ and $Zn_2(\mathbf{1,3})_2(Et)_2$ exhibited a distorted tetrahedral geometry around the metal centre, consistent with a τ_4 value close to 1

Scheme 1 Metal-mediated degradation mechanism of PLA into methyl lactate via transesterification with MeOH, where R denotes the growth polymer chain.

Scheme 2 Schiff-base ligand preparation and their complexation to Zn(II) to afford a series of mono-, $Zn(\mathbf{1–3})_2$, and analogous dimeric, $Zn_2(\mathbf{1–3})_2(Et)_2$, complexes.

Table 1 Selected bond angles for Zn(**1–3**)$_2$ and Zn$_2$(**1–3**)$_2$(Et)$_2$ with calculated τ_4 values. Ideal tetrahedral geometry corresponds to $\tau_4 = 1$

Init.	Bond	Bond angle/°	τ_4
Zn(**1**)$_2$	O(1)–Zn(1)–N(2), O(2)–Zn(1)–N(1)	115.26(8), 155.48(8)	0.92
Zn(**2**)$_2$	O(2)–Zn(1)–N(1), N(1)–Zn(1)–N(2)	113.54(5), 126.19(5)	0.85
Zn(**3**)$_2$	O(2)–Zn(1)–N(1), O(1)–Zn(1)–N(2)	119.02(6), 121.68(6)	0.85
Zn$_2$(**1**)$_2$(Et)$_2$	C(1)–Zn(1)–O(1), C(1)–Zn(1)–N(2)	124.10(15), 132.40(16)	0.73
Zn$_2$(**2**)$_2$(Et)$_2$	C(1)–Zn(1)–N(1), C(1)–Zn(1)–O(1)	124.86(10), 129.61(10)	0.75
Zn$_2$(**3**)$_2$(Et)$_2$	C(1)–Zn(1)–O(1), C(1)–Zn(1)–N(1)	125.13(8), 134.65(8)	0.71

(Table 1). XRD analysis revealed Zn$_2$(**1–3**)$_2$(Et)$_2$ to adopt a phenoxy-bridged dimeric structure. In all instances, the Zn–O bond lengths increased between mono- and dimeric analogues, consistent with the observed shift from a 2c–2e$^-$ to 3c–2e$^-$ bonding system {Zn(**2**)$_2$: Zn(1)–O(1) = 1.9297(11) Å, Zn$_2$(**2**)$_2$(Et)$_2$: Zn(1)–O(1) = 2.0293(17) Å}. A Zn(1)–N(2) bond length of *ca.* 2 Å confirmed the retention of the imine functionality on coordination to Zn(II) for all complexes (Fig. 1), consistent with previously reported Zn(II)-complexes.[45] This was reaffirmed by ^{1}H NMR spectroscopic analysis, which exhibited a characteristic singlet peak at *ca.* 8 ppm corresponding to a HC=N resonance. Additionally, the absence of a singlet resonance around 14 ppm, present in the isolated ligand, confirmed the loss of O–H functionality on coordination to the Zn(II) centre (Fig. 1). In all cases, ^{1}H NMR spectra suggested identical ligand coordination environments for each

Zn(II)-complex in solution, with the exception of Zn$_2$(**1**)$_2$(Et)$_2$. Four singlet peaks corresponding to [t]Bu resonances were observed for Zn$_2$(**1**)$_2$(Et)$_2$, suggesting multiple species present in solution. Diffusional ordered spectroscopy (DOSY) NMR analysis indicated the presence of two distinct species in solution, as a consequence of the Schlenk type equilibrium, corresponding to Zn(**1**)$_2$ and Zn(**1**)Et with diffusion constants (*D*) of 0.6×10^{-9} and 0.8×10^{-9} m^2 s^{-1} respectively (see ESI†). Zn(**1**)Et, instead of Zn$_2$(**1**)$_2$Et$_2$, is proposed due to the large *D* observed.

A comparison between the ^{1}H NMR spectra of Zn$_2$(**2–3**)$_2$Et$_2$ with their respective monomeric counterparts indicates no presence of the homoleptic species, and thus are not susceptible to the Schlenk type equilibrium noted for Zn$_2$(**1**)$_2$(Et)$_2$. It is proposed Zn(**1**)Et is stabilised by the steric bulk of **1**H. For Zn$_2$(**1–3**)$_2$(Et)$_2$, resonances in the region of *ca.* δ 0.5–1.5 ppm

Fig. 1 Solid-state structures of Zn(**1–3**)$_2$ (top left to right) and Zn$_2$(**1–3**)$_2$(Et)$_2$ (bottom left to right). Ellipsoids shown at 30% probability, with all hydrogen atoms, and one toluene molecule for Zn(**1–2**)$_2$, omitted for clarity.

confirmed coordination of Et- to Zn(II) in solution, consistent with XRD analysis. Interestingly, *trans*-Et coordination was observed in $Zn_2(2–3)_2(Et)_2$ compared to *cis*-Et in $Zn_2(1)_2(Et)_2$. This is likely a consequence of reduced steric demand in $Zn_2(2–3)_2(Et)_2$ compared to $Zn_2(1)_2(Et)_2$. $^{13}C\{^1H\}$ NMR analysis was consistent with XRD and ^1H NMR data, although poor peak resolution was observed for both $Zn(2)_2$ and $Zn(2)_2(Et)_2$, indicative of fluxionality on the $^{13}C\{^1H\}$ NMR timescale. All Zn(II)-complexes were generally in good agreement with elemental analysis (EA) data obtained. The scalability of these complexes was also demonstrated, producing 14.6 g of $Zn(2)_2$ in exceptional yield (87%).

Polymerisation

All Zn(II)-complexes were trialled for the polymerisation of *rac*-lactide (*rac*-LA) under both industrially preferred conditions in the absence of solvent at elevated temperatures (Tables 2 and 3) and in solution (Table 4). Catalysts that operate under industrially viable conditions are desirable since they remove the need for solvents, which are typically a significant source of waste.[45–49] The lactide monomer, *rac*-LA, was recrystallised from toluene once prior to use, and benzyl alcohol was employed as a co-initiator. Conversion was determined *via* analysis of the methine region (*ca.* δ 4.9–5.2 ppm) by means of ^1H NMR spectroscopy. All initiators demonstrated rapid polymerisation at 130 °C, achieving high conversion within minutes {[*rac*-LA]:[Init]:[BnOH] = 300:1:1} (Table 2). The reduction in activity of $Zn(1)_2$ compared to $Zn(2–3)_2$ could likely be attributed to reduced steric bulk of the substituted phenoxy-fragment. In all instances, $Zn_2(1–3)_2(Et)_2$ exhibited superior activity compared to their respective monomeric counterparts. It is proposed $Zn(1–3)_2$ operate *via* an activated

Table 2 Polymerisation of *rac*-LA at 130 °C using Zn(II)-complexes

Init.	[*rac*-LA]:[I]:[BnOH]	Time/min	Conv.[a]/%	$M_{n/theo}$[b]	M_n[c]	$Đ$[c]	P_r[d]
$Zn(1)_2$	300:1:1	9	69	29 900	16 650	1.86	0.56
	300:1:6	10	90	6600	13 000	1.46	0.54
$Zn(2)_2$	300:1:1	2	78	33 800	26 600	1.75	0.54
$Zn(3)_2$	300:1:1	2	88	38 100	43 700	1.98	0.54
$Zn_2(1)_2Et_2$	300:1:1	2	88	38 100	25 350	1.99	0.55
$Zn_2(2)_2Et_2$	300:1:1	<1	72	31 200	17 000	1.67	0.54
$Zn_2(3)_2Et_2$	300:1:1	2	96	41 600	46 600	2.20	0.53

Conditions: *rac*-LA, solvent free (130 °C). [a] Determined *via* ^1H NMR spectroscopy. [b] Theoretical average number molecular weight (M_n) dependent on conversion and co-initiator added {$(M_{r,LA} \times 3 \times \%_{conv}) + M_{n,BnOH}$}. [c] Determined *via* GPC analysis (in THF). [d] Determined *via* homonuclear decoupled NMR spectroscopy. Note {[I]:[BnOH] = 1:1} corresponds to 1 equivalent of BnOH per Zn centre.

Table 3 Polymerisation of *rac*-LA at 180 °C using Zn(II)-complexes

Init.	[*rac*-LA]:[I]:[BnOH]	Time/min	Conv.[a]/%	$M_{n/theo}$[b]	M_n[c]	$Đ$[c]	P_r[d]
$Zn(1)_2$	3000:1:10	18	47	20 400	63 450	1.96	0.58
$Zn(2)_2$	3000:1:10	<1	55	23 850	124 400	1.95	0.58
$Zn(3)_2$	3000:1:10	10	72	31 200	116 800	2.04	0.58
$Zn_2(1)_2Et_2$	3000:1:10	<1	92	39 850	61 200	2.04	0.58
$Zn_2(2)_2Et_2$	3000:1:10	<1	94	40 700	54 550	1.91	0.56
$Zn_2(3)_2Et_2$	3000:1:10	<1	88	38 100	40 000	1.83	0.58

Conditions: *rac*-LA, solvent free (180 °C). [a] Determined *via* ^1H NMR spectroscopy. [b] Theoretical average number molecular weight (M_n) dependent on conversion and co-initiator added {$(M_{r,LA} \times 3 \times \%_{conv}) + M_{n,BnOH}$}. [c] Determined *via* GPC analysis (in THF). [d] Determined *via* homonuclear decoupled NMR spectroscopy. Note {[I]:[BnOH] = 1:1} corresponds to 1 equivalent of BnOH per Zn centre.

Table 4 Polymerisation of *rac*-LA at 80 °C using Zn(II)-complexes

Init.	[*rac*-LA]:[I]:[BnOH]	Time/h	Conv.[a]/%	$M_{n/theo}$[b]	M_n[c]	$Đ$[c]	P_r[d]
$Zn(1)_2$	100:1:1	2	70	10 200	8800	1.27	0.46
$Zn(2)_2$	100:1:1	0.50	95	13 800	12 600	1.83	0.51
$Zn(3)_2$	100:1:1	0.50	96	13 950	16 200	1.73	0.50
$Zn2(1)_2Et_2$	100:1:1	0.17	92	13 350	12 600	1.21	0.53
$Zn2(2)_2Et_2$	100:1:1	0.17	96	13 900	12 650	1.42	0.55
	100:1:1	30[e]	83	12 050	11 900	1.22	0.59
$Zn2(3)_2Et_2$	100:1:1	0.17	96	13 900	12 000	1.24	0.47
	100:1:1	24[e]	99	14 350	10 850	1.44	0.58

Conditions: rac-LA, solvent (toluene, 80 °C). [a] Determined *via* ^1H NMR spectroscopy. [b] Theoretical average number molecular weight (M_n) dependent on conversion and co-initiator added {$(M_{r,LA} \times \%_{conv}) + M_{n,BnOH}$}. [c] Determined *via* GPC analysis (in THF). [d] Determined *via* homonuclear decoupled NMR spectroscopy. [e] RT. Note {[I]:[BnOH] = 1:1} corresponds to 1 equivalent of BnOH per Zn centre.

monomer mechanism, whilst $Zn_2(1–3)_2(Et)_2$ operate *via* a coordination- insertion mechanism once the labile Et- group is displaced by –OBn. To investigate this the stability of $Zn(1)_2$ and $Zn_2(3)_2(Et)_2$ in BnOH was studied. ^{1}H NMR analysis revealed the former to be stable, whilst the latter converted to the corresponding BnO– analogue *via* elimination of the terminal –Et to afford dissolved ethane (see ESI†), consistent with the emergence of a single CH_3 resonance at *ca.* $\delta = 0.80$ ppm, as expected. These results are compatible with the respective suggested mechanisms. $Zn(3)_2$ and $Zn_2(3)_2(Et)_2$ achieved the highest conversions of 88% and 96% respectively within 2 minutes, suggesting reduced sterics dominates electron withdrawing inductive effects in both subseries. All initiators offered moderate number average molecular weight (M_n) control, with broad dispersities ($Đ = 1.67–2.20$) observed under these conditions. Reduced M_n control may also be due to rapid polymerisation (<1 min) inhibiting homogeneity, thus preventing optimal initiation. $Zn(1)_2$ was repeated at {[*rac*-LA] : [Init] : [BnOH] = 300 : 1 : 6} to afford PLA of sufficiently low M_n weight for end group characterisation. MALDI-ToF analysis confirmed the polymer (Table 2, entry 2) to be –OBn and –H end-capped with multiple series present suggesting poor polymerisation control, consistent with GPC data. For all $Zn(II)$-initiators, polymerisation of *rac*-LA afforded atactic PLA ($P_r \approx 0.5$). Whilst maintaining a constant *rac*-LA : co-initiator ratio at reduced catalyst loading {[*rac*-LA] : [Init] : [BnOH] = 3000 : 1 : 10} (Table 3), increasing the temperature to 180 °C resulted in a shift to very slight heterotactic PLA ($P_r = 0.58$). Generally, accelerated polymerisation (<1 min) was observed at higher temperatures, with the exception of $Zn(1,3)_2$. $Zn_2(1–3)_2(Et)_2$ exhibited superior activity compared to their monomeric analogues, consistent with observations at 130 °C. At 3000 : 1 : 10, moderate M_n control and broad dispersities ($Đ = 1.83–2.04$) were observed, consistent with observations at 130 °C. However, GPC analysis revealed both $Zn(2–3)_2$ produced PLA of significantly higher M_n than predicted. Superior M_n control was achieved at lower polymerisation temperatures (80 °C) in solution {[*rac*-LA] : [Init] : [BnOH] = 100 : 1 : 1} (Table 4), producing atactic PLA ($P_r \approx 0.5$) with broad dispersities ($Đ = 1.21–1.83$). All $Zn(II)$-initiators achieved high conversion (≥92%) within 10 to 30 minutes, with the exception of $Zn(1)_2$, which achieved 70% conversion after 2 h, consistent with observations at 130 and 180 °C. MALDI-ToF analysis revealed the polymer (Table 4, entry 1) to be BnO– and –H end-capped, with molecular weight consistent with GPC and observations in the melt (see ESI†). A second series of lower intensity was observed corresponding to transesterified polymer, an initial indication of the catalysts propensity to facilitate PLA degradation.

Interestingly, all dimers exhibited exceptional M_n control, which is considerably poorer under extended periods of polymerisation ($Đ = 1.63–2.21$ after 2 h), presumably due to detrimental transesterification. It was envisaged the *trans*-Et-configuration in $Zn_2(2–3)_2(Et)_2$ would facilitate coordination of initiated polymer chains above and below the plane of the $Zn(II)–O–Zn(II)$ framework, resulting in superior monomer selectivity. Therefore, the solution polymerisations were

repeated at RT. Both $Zn_2(2–3)_2(Et)_2$ exhibited a shift to very slight heterotactic PLA ($P_r = 0.58–0.59$) and narrower dispersities ($Đ = 1.22–1.44$) compared to 80 °C, suggesting enhanced control at the expense of high catalyst activity, consistent with the literature.[45] $Zn_2(2)_2(Et)_2$ displayed exceptional M_n control under these conditions (M_n, = 11 900; $M_{n,theo}$ = 12 050). Reactivity trends were consistent with those observed in the melt at 130 °C, with $Zn_2(3)_2(Et)_2$ achieving 99% conversion within 24 h. Under solution conditions, it is tentatively suggested the original dimeric framework of $Zn_2(2–3)_2Et_2$, is retained, although there is existing literature precedent for benzoxy bridged dinuclear $Zn(II)$-initiators.[50–53] In light of DOSY NMR analysis, presence of the Schlenk type equilibrium for $Zn_2(1)_2Et_2$ inhibits the rationale for the proposed species. In summary, all $Zn(II)$-initiators exhibited high catalyst activity in the polymerisation of *rac*-LA, consistent with previous examples in the literature.[41,42,45,46,50–63]

Polymerisation kinetics

Generally, $Zn_2(1–3)_2Et_2$ outperformed their monomeric counterparts under both melt and solution conditions. A mono- *vs.* dimeric system kinetic study was envisaged but not possible due to the extremely high activity of the latter. To this end, $Zn(1)_2$ and $Zn(2)_2$ were chosen to better understand the impact of steric and electronic effects on polymerisation activity in solution (Fig. 2 and 3). The consumption of *rac*-LA was shown to adopt first-order kinetics as demonstrated by the linear relationship of $\ln([LA]_0/[LA]_t)$ against time (Fig. 2). $Zn(1)_2$ and $Zn(2)_2$ exhibited apparent rate constants (k_{app}) of 0.0068 and 0.081 min^{−1} respectively, indicating reduced sterics, coupled with a more electron withdrawing ligand, affords enhanced polymerisation activity with statistical significance. GPC analysis of the retained aliquots for $Zn(1)_2$ confirmed the polymerisation to be well controlled and living, demonstrated by a linear increase in M_n with conversion, whilst retaining a narrow $Đ$ range (Fig. 3).
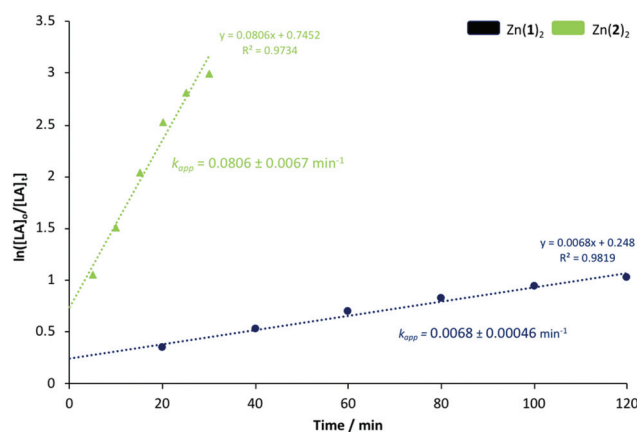

Fig. 2 First-order logarithmic plot for the polymerisation of *rac*-LA at 80 °C in toluene {[*rac*-LA] : [I] : [BnOH] = 100 : 1 : 1} using $Zn(1)_2$ and $Zn(2)_2$. Note $[LA]_0 = 0.69$ mol dm^{−3}.
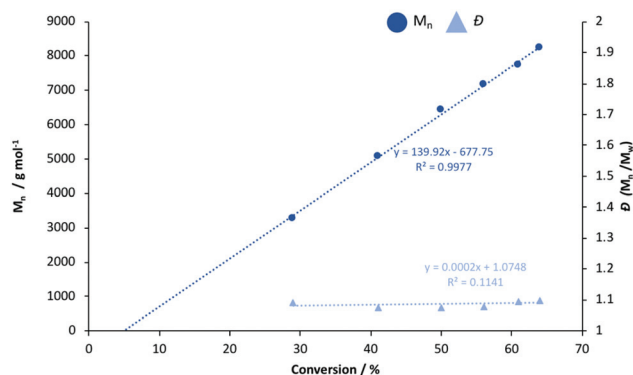
Fig. 3 M_n and $Đ$ against conversion for the solution polymerisation of *rac*-LA in toluene at 80 °C using Zn(**1**)$_2$.

Degradation

All Zn(II)-complexes were investigated in the metal-mediated degradation of PLA into methyl lactate (Me-LA) in solution between 50–80 °C (Table 5). In addition to Me-LA being a green alternative to traditional petrochemical based solvents, it can also be directly converted to lactide and is therefore a potentially valuable chemical to the PLA supply chain.[24,25,64] Commercially available polymer (0.25 g, Vegware™, PLA cup, M_n = 45 510 g mol^{-1}) and catalyst were dissolved in THF under Ar, with heat and stirring assisting dissolution. MeOH was then added, and the conversion to Me-LA was determined *via* ^{1}H NMR analysis of the methine region (*ca.* δ 4.2–5.2 ppm). We have previously demonstrated the production of Me-LA proceeds *via* a two-step process through the intermediate formation of chain-end groups (see ESI†).[41] As such, the methine groups can be categorised as internal (int), chain end (CE) and those corresponding directly to the alkyl lactate (Me-LA), as denoted in Table 5. In general, reasonably good catalyst activity was observed under milder reaction conditions compared to previously reported recycling systems.[14,15,18,33,37,38,43,65–69] In all instances, an increase in temperature coincided with

higher Me-LA yield (Y_{Me-LA}) and shorter reaction times, consistent with the literature.[35,41,43] Zn(**2**)$_2$ exhibited superior activity compared to Zn(**1**,**3**)$_2$ at 50 °C, suggesting inductive effects dominate, whilst Zn(**1**)$_2$ exhibited the lowest degradation activity, both consistent with polymerisation results (Table 3). As noted previously, a shift to the corresponding dimeric analogue, Zn$_2$(**1**)$_2$(Et)$_2$, coincided with superior activity at both 50 and 80 °C, with the exception of Zn(**2–3**)$_2$. This was likely due to reduced sterics in the latter two rendering the dimeric counterparts more susceptible to decomposition at 50 °C, resulting in deactivation. It is suggested this effect was remediated by an increase in rate of reaction at 80 °C. Indeed, both Zn(**2–3**)$_2$ and Zn$_2$(**3**)$_2$(Et)$_2$ achieved 100% conversion to Me-LA within 8 h at 80 °C. Overall, mass transfer limitations due to polymer particle size and stirring speed were considered to be negligible based on previously reported work by McKeown *et al.*[41] on an analogous Zn(II)-imino monophenolate system.

Degradation kinetics

Both Zn(**2**)$_2$ and Zn(**3**)$_3$ were chosen for further analysis owing to their high degradation activity, stability and potential scalability. To ensure sufficiently short reaction times, degradation reactions were repeated under identical conditions at 80 °C (Table 5). Reaction progress was monitored hourly by taking aliquots for ^{1}H NMR (CDCl$_3$) analysis of the methine region (Fig. 4). Zn(**2–3**)$_2$ achieved comparable yields of Me-LA after 8 h, although 100% conversion to Me-LA was not achieved as pre-
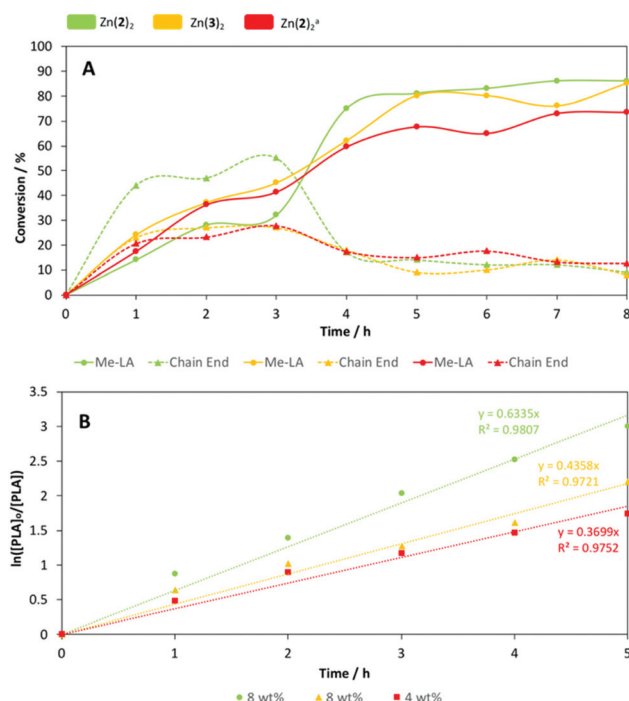
Table 5 Degradation of PLA into Me-LA using Zn(II)-complexes[a,b]

Init.	Time/h	T/°C	Y_{Me-LA}/%	Y_{CE}/%	X_{int}/%
Zn(**1**)$_2$	18	50	41	22	37
	8	80	54	18	28
Zn(**2**)$_2$	18	50	88	6	6
	8	80	100	0	0
Zn(**3**)$_2$	18	50	77	13	10
	8	80	100	0	0
Zn$_2$(**1**)$_2$(Et)$_2$	18	50	57	17	26
	8	80	81	11	8
Zn$_2$(**2**)$_2$(Et)$_2$	18	50	71	13	16
	8	80	88	7	5
Zn$_2$(**3**)$_2$(Et)$_2$	18	50	52	21	27
	8	80	100	0	0

[a] Reaction conditions: 0.25 g of PLA, V_{THF} : V_{MeOH} = 4 : 1, [Zn(**1–3**)$_2$/ Zn$_2$(**1–3**)$_2$(Et)$_2$] = 8 wt% cat. loading, n_{MeOH} : n_{ester} = 7 : 1. [b] Me-LA and oligomer yield (Y_{Me-LA} and Y_{CE} respectively) determined by ^{1}H NMR upon solvent (THF) removal.

Fig. 4 (A) Vegware PLA cup degradation plot of conversion *vs.* time with Zn(**2–3**)$_2$ at 8 wt% in THF at 80 °C. [a] [Zn(**2**)$_2$] = 4 wt%. (B) Pseudo-first-order logarithmic plots for the degradation of Vegware PLA cup with Zn(**2–3**)$_2$ in THF at 80 °C. Line of best fit constrained to pass through the origin.

Table 6 PLA cup degradation with Zn(2–3)$_2$ in THF at 80 °C^{a,b,c}

Init.	$Y_{\text{Me-LA}}$ ^{b}/%	k_{app}/h^{-1}
Zn(2)$_2$	87	0.63 ± 0.051
Zn(3)$_2$	82	0.44 ± 0.029
Zn(2)$_2$ ^{d}	78	0.37 ± 0.021

^{a} Reaction conditions: 0.25 g of PLA, $V_{\text{THF}} : V_{\text{MeOH}}$ = 4 : 1, [Zn(2–3)$_2$] = 8 wt% cat. loading, $n_{\text{MeOH}} : n_{\text{ester}}$ = 7 : 1. ^{b} Maximum Me-LA conversion ($Y_{\text{Me-LA}}$) determined *via* ^{1}H NMR (CDCl$_3$) analysis after 8 h upon solvent (THF) removal. ^{c} Error associated with k_{app} using linear regression. ^{d} [Zn(2)$_2$] = 4 wt% cat. loading.

viously noted (Table 5). PLA degradation using Zn(2)$_2$ was also tested at 4 wt%. Interestingly, at a lower catalyst loading, a higher Me-LA conversion was achieved within 3 h compared to 8 wt%, suggesting preferential transesterification of oligomer compared to polymer. However, the general degradation profile was retained, albeit with a less severe rapid conversion event, likely due to a shift in transesterification selectivity. As expected, a lower overall Me-LA conversion (78%) was observed compared to Zn(2)$_2$ at 8 wt%. In all instances, fluctuations in Me-LA and oligomer yield ($Y_{\text{Me-LA}}$ and Y_{CE} respectively) can likely be attributed to an equilibrium process.[70] In accordance to kinetic work by Mckeown *et al.*,[41] PLA consumption was presumed to adopt pseudo-first-order kinetics (Fig. 2b). Thus, the gradient of the logarithmic plot is equivalent to the apparent rate constant, k_{app} (Table 6). Zn(2–3)$_2$ exhibited k_{app} values of 0.63 ± 0.051 and 0.44 ± 0.029 h^{-1} respectively at 8 wt%, indicating reduced sterics and electronics imparts a statistically significant reduction in activity. For Zn(2)$_2$, a shift to 4 wt% coincided with a statistically significant reduction in k_{app} (0.37 ± 0.021 h^{-1}) as expected.

Conclusion

A series of novel mono- and dimeric Zn(II)-Schiff-base complexes were successfully synthesised and fully characterised. Their application in the ROP of *rac*-LA to produce biocompatible atactic PLA was demonstrated in both solution and under industrially preferred melt conditions, albeit with generally poor M_n control and broad dispersities (Đ). Additionally, their capacity to facilitate PLA degradation into Me-LA under mild conditions was shown. Zn(2)$_2$ and Zn(3)$_2$ emerged as the outstanding candidates, with both achieving 100% conversion to Me-LA within 8 h at 80 °C in THF. Further degradation kinetic analysis revealed Zn(2–3)$_2$ to possess k_{app} values of 0.63 ± 0.051 and 0.44 ± 0.029 h^{-1} respectively at 8 wt%, indicating steric and electronic effects have a statistically significant impact on degradation activity. A statistically significant reduction in k_{app} was observed for Zn(2)$_2$ between 8 and 4 wt%.

Experimental

An exemplar synthesis is provided below, see ESI† for full details.

Ligand

1H: To a solution of 3,5-di-*tert*-butyl-2-hydroxybenzaldehyde (4.68 g. 20 mmol) dissolved in MeOH (50 mL), aniline (1.86 g, 1.82 mL, 20 mmol) was added with stirring. The reaction mixture was then left to stir at RT for 18 h, affording a yellow solid product. The product was then separated by filtration, washed with MeOH (5 × 5 mL) and dried *in vacuo*. Yield = 4.74 g, 77%.

Zn(II)-Complex

Zn(1)$_2$: To a solution of **1H** (0.62 g, 2 mmol) dissolved in anhydrous toluene (10 mL), ZnEt$_2$ (1 M in hexane, 1 mmol) was added dropwise with stirring. After complete addition, the solution was stirred at RT for 15 minutes before being left to stand for 1 h. The solvent was then removed *via* cannula filtration and the desired Zn(II) complex was recrystallised from hexane as yellow crystals. Yield = 0.50 g, 73%.

Polymerisation

Polymerisations were conducted in a Youngs ampoule under argon. *rac*-LA was recrystallised once from toluene prior to use. All melt polymerisations were performed in the absence of solvent. The reaction commenced on melting of the monomer and deemed finished once a polymer melt of sufficient viscosity stopped the stirrer bar. The reaction was then quenched in air and the product dissolved in DCM (20 mL) with stirring. The solvent was then removed *in vacuo* and a crude ^{1}H NMR spectrum of the polymer was obtained. The polymer was then washed with copious amounts of MeOH (100 mL) to remove initiator and any unreacted monomer, dried *in vacuo* and retained for materials characterisation. Solution polymerisations were conducted in anhydrous toluene (10 mL) using the purification method described for the melt.

Degradation

All reactions were performed in a Youngs ampoule under argon. The flask was loaded with Zn(II) catalyst (8 wt% – 1 mol% relative to PLA ester linkages, 0.02 g) in a Glovebox to which PLA (0.25 g, Vegware™, PLA cup, M_n = 45 510 g mol^{-1}) was added under a flow of argon. The polymer was then dissolved in THF (4 mL), with heating and stirring assisting dissolution. The flask was then submerged in a preheated oil bath (50 or 80 °C) to which MeOH (1 mL) was added. Aliquots were taken for ^{1}H NMR (CDCl$_3$) analysis of the methine region. After the reaction, the solvent was removed *in vacuo* and the residual methyl lactate (Me-La) was analysed further.

Conflicts of interest

The authors declare no conflict of interest.

Acknowledgements

References

1 European Bioplastics, *Facts and Fig.* 2016, http://docs.europeanbioplastics.org/2016/publications/EUBP_Facts_and_Figures_2017.pdf, (Accessed: 30th October 2018).

2 R. C. Thompson, C. J. Moore, F. S. vom Saal and S. H. Swan, *Philos. Trans. R. Soc., B*, 2009, **364**, 2153–2166.

3 Y. Zhu, C. Romain and C. K. Williams, *Nature*, 2016, **540**, 354–362.

4 Ellen MacArthur Foundation, *The New Plastics Economy: Rethinking the future of plastics*, 2016, https://www.ellenmacarthurfoundation.org/publications/the-new-plastics-economy-rethinking-the-future-of-plastics, (Accessed: 7th January 2019).

5 M. Rabnawaz, I. Wyman, R. Auras and S. Cheng, *Green Chem.*, 2017, **19**, 4737–4753.

6 R. Geyer, J. R. Jambeck and K. L. Law, *Sci. Adv.*, 2017, **3**, 1–5.

7 Ellen MacArthur Foundation, *The New Plastics Economy: Catalysing Action*, 2016, https://www.ellenmacarthurfoundation.org/assets/downloads/New-Plastics-Economy_Catalysing-Action_13-1-17.pdf, (Accessed: 9th January 2019).

8 E. T. H. Vink, K. R. Rábago, D. A. Glassner, B. Springs, R. P. O'Connor, J. Kolstad and P. R. Gruber, *Macromol. Biosci.*, 2004, **4**, 551–564.

9 E. T. H. Vink, D. A. Glassner, J. Kolstad, R. J. Wooley and R. P. O'Connor, *Biotechnology*, 2007, **3**, 58–81.

10 M. Dusselier, P. V. Wouwe, A. Dewaele, P. A. Jacobs and B. F. Sels, *Science*, 2015, **349**, 78–80.

11 R. De Clercq, M. Dusselier, C. Poleunis, D. P. Debecker, L. Giebeler, S. Oswald, E. Makshina and B. F. Sels, *ACS Catal.*, 2018, **8**, 8130–8139.

12 T. P. Haider, C. Völker, J. Kramm, K. Landfester and F. R. Wurm, *Angew. Chem., Int. Ed.*, 2019, **58**, 50–62.

13 J. Hopewell, R. Dvorak and E. Kosior, *Philos. Trans. R. Soc., B*, 2009, **364**, 2115–2126.

14 H. Tsuji, H. Daimon and K. Fujie, *Biomacromolecules*, 2003, **4**, 835–840.

15 Y. Aoyagi, K. Yamashita and Y. Doi, *Polym. Degrad. Stab.*, 2002, **76**, 53–59.

16 Y. Tokiwa, B. P. Calabia, C. U. Ugwu and S. Aiba, *Int. J. Mol. Sci.*, 2009, **10**, 3722–3742.

17 P. Coszach, J.-C. Bogaert and J. Willocq, *US Pat*, 8431683B2, 2013.

18 H. Tsuji, T. Saeki, T. Tsukegi, H. Daimon and K. Fujie, *Polym. Degrad. Stab.*, 2008, **93**, 1956–1963.

19 V. Piemonte and F. Gironi, *J. Polym. Environ.*, 2013, **21**, 313–318.

20 C. F. Van Nostrum, T. F. J. Veldhuis, G. W. Bos and W. E. Hennink, *Polymer*, 2004, **45**, 6779–6787.

21 F. Codari, S. Lazzari, M. Soos, G. Storti, M. Morbidelli and D. Moscatelli, *Polym. Degrad. Stab.*, 2012, **97**, 2460–2466.

22 S. Lazzari, F. Codari, G. Storti, M. Morbidelli and D. Moscatelli, *Polym. Degrad. Stab.*, 2014, **110**, 80–90.

23 K. Odelius, A. Höglund, S. Kumar, M. Hakkarainen, A. K. Ghosh, N. Bhatnagar and A. C. Albertsson, *Biomacromolecules*, 2011, **12**, 1250–1258.

24 C. T. Bowmer, R. N. Hooftman, A. O. Hanstveit, P. W. M. Venderbosch and N. van der Hoeven, *Chemosphere*, 1998, **37**, 1317–1333.

25 C. S. M. Pereira, V. M. T. M. Silva and A. E. Rodrigues, *Green Chem.*, 2011, **13**, 2658–2671.

26 J. J. Bozell and G. R. Petersen, *Green Chem.*, 2010, **12**, 539–554.

27 Y. Fan, C. Zhou and X. Zhu, *Catal. Rev.: Sci. Eng.*, 2009, **51**, 293–324.

28 J. Payne, P. McKeown and M. D. Jones, *Polym. Degrad. Stab.*, 2019, **165**, 170–181.

29 M. Dusselier, P. V. Wouwe, A. Dewaele, E. Makshina and B. F. Sels, *Energy Environ. Sci.*, 2013, **6**, 1415–1442.

30 L. D. Brake, *US Pat*, 5264617, 1993.

31 X. Song, X. Zhang, H. Wang, F. Liu, S. Yu and S. Liu, *Polym. Degrad. Stab.*, 2013, **98**, 2760–2764.

32 X. Song, Z. Bian, Y. Hui, H. Wang, F. Liu and S. Yu, *Polym. Degrad. Stab.*, 2019, **168**, 108937–108944.

33 X. Song, H. Wang, X. Zheng, F. Liu and S. Yu, *J. Appl. Polym. Sci.*, 2014, **131**, 40817–40823.

34 F. Nederberg, E. F. Connor, T. Glausser and J. L. Hedrick, *Chem. Commun.*, 2001, 2066–2067.

35 F. A. Leibfarth, N. Moreno, A. P. Hawker and J. D. Shand, *J. Polym. Sci., Part A: Polym. Chem.*, 2012, **50**, 4814–4822.

36 L. Monsigny, J.-C. Berthet and T. Cantat, *ACS Sustainable Chem. Eng.*, 2018, **6**, 10481–10488.

37 S. Westhues, J. Idel and J. Klankermayer, *Sci. Adv.*, 2018, **4**, 1–8.

38 E. M. Krall, T. W. Klein, R. J. Andersen, A. J. Nett, R. W. Glasgow, D. S. Reader, B. C. Dauphinais, S. P. McIlrath, A. A. Fischer, M. J. Carney, *et al.*, *Chem. Commun.*, 2014, **50**, 4884–4887.

39 E. L. Whitelaw, M. G. Davidson and M. D. Jones, *Chem. Commun.*, 2011, **47**, 10004–10006.

40 C. Fliedel, D. Vila-Viçosa, M. J. Calhorda, S. Dagorne and T. Avilés, *ChemCatChem*, 2014, **6**, 1357–1367.

41 L. A. Román-Ramírez, P. Mckeown, M. D. Jones and J. Wood, *ACS Catal.*, 2019, **9**, 409–416.

42 P. McKeown, L. A. Román-Ramírez, S. Bates, J. Wood and M. D. Jones, *ChemSusChem*, 2019, **12**, 5233–5238.

43 R. Petrus, D. Bykowski and P. Sobota, *ACS Catal.*, 2016, **6**, 5222–5235.

44 H. Liu, X. Song, F. Liu, S. Liu and S. Yu, *J. Polym. Res.*, 2015, **22**, 135–141.

45 P. McKeown, S. N. McCormick, M. F. Mahon and M. D. Jones, *Polym. Chem.*, 2018, **9**, 5339–5347.

46 M. Fuchs, S. Schmitz, P. M. Schäfer, T. Secker, A. Metz, A. N. Ksiazkiewicz, A. Pich, P. Kögerler, K. Y. Monakhov and S. Herres-Pawlis, *Eur. Polym. J.*, 2020, **122**, 109302–109308.

47 P. M. Schäfer, M. Fuchs, A. Ohligschläger, R. Rittinghaus, P. McKeown, E. Akin, M. Schmidt, A. Hoffmann, M. A. Liauw, M. D. Jones and S. Herres-Pawlis, *ChemSusChem*, 2017, **10**, 3547–3556.

48 J. Börner, I. Dos Santos Vieira, A. Pawlis, A. Döring, D. Kuckling and S. Herres-Pawlis, *Chem. – Eur. J.*, 2011, **17**, 4507–4512.

49 J. Börner, U. Florke, K. Huber, A. Döring, D. Kuckling and S. Herres-Pawlis, *Chem. – Eur. J.*, 2009, **15**, 2362–2376.

50 H.-Y. Chen, H.-Y. Tang and C.-C. Lin, *Macromolecules*, 2006, **39**, 3745–3752.

51 H.-L. Chen, H.-J. Chuang, B.-H. Huang and C.-C. Lin, *Inorg. Chem. Commun.*, 2013, **35**, 247–251.

52 W.-C. Hung, Y. Huang and C.-C. Lin, *J. Polym. Sci., Part A: Polym. Chem.*, 2008, **46**, 6466–6476.

53 D. Jędrzkiewicz, G. Adamus, M. Kwiecień, Ł. John and J. Ejfler, *Inorg. Chem.*, 2017, **56**, 1349–1365.

54 M. Cheng, A. B. Attygalle, E. B. Lobkovsky and G. W. Coates, *J. Am. Chem. Soc.*, 1999, **121**, 11583–11584.

55 M. H. Chisholm, J. C. Huffman and K. Phomphrai, *J. Chem. Soc., Dalton Trans.*, 2001, 222–224.

56 M. H. Chisholm, J. Gallucci and K. Phomphrai, *Inorg. Chem.*, 2002, **41**, 2785–2794.

57 M. H. Chisholm and K. Phomphrai, *Inorg. Chim. Acta*, 2003, **350**, 121–125.

58 B. M. Chamberlain, M. Cheng, D. R. Moore, T. M. Ovitt, E. B. Lobkovsky and G. W. Coates, *J. Am. Chem. Soc.*, 2001, **123**, 3229–3238.

59 C. Kan, J. Hu, Y. Huang, H. Wang and H. Ma, *Macromolecules*, 2017, **50**, 7911–7919.

60 S. Abbina and G. Du, *ACS Macro Lett.*, 2014, **3**, 689–692.

61 D. E. Stasiw, A. M. Luke, T. Rosen, A. B. League, M. Mandal, B. D. Neisen, C. J. Cramer, M. Kol and W. B. Tolman, *Inorg. Chem.*, 2017, **56**, 14366–14372.

62 A. Thevenon, C. Romain, M. S. Bennington, A. J. P. White, H. J. Davidson, S. Brooker and C. K. Williams, *Angew. Chem., Int. Ed.*, 2016, **55**, 8680–8685.

63 C. K. Williams, L. E. Breyfogle, S. K. Choi, W. Nam, V. G. Young, M. A. Hillmyer and W. B. A. Tolman, *J. Am. Chem. Soc.*, 2003, **125**, 11350–11359.

64 P. P. Upare, Y. K. Hwang, J.-S. Chang and D. W. Hwang, *Ind. Eng. Chem. Res.*, 2012, **51**, 4837–4842.

65 A. C. Sanchéz and S. R. Collinson, *Eur. Polym. J.*, 2011, **47**, 1970–1976.

66 C. Alberti, N. Damps, R. R. R. Meißner, M. Hofmann, D. Rijono and S. Enthaler, *Adv. Sustainable Syst.*, 2020, **4**, 1900081.

67 C. Alberti, N. Damps, R. R. R. Meißner and S. Enthaler, *ChemistrySelect*, 2019, **4**, 6845–6848.

68 A. Plichta, P. Lisowska, A. Kundys, A. Zychewicz, M. Dębowski and F. Florjańczyk, *Polym. Degrad. Stab.*, 2014, **108**, 288–296.

69 K. Hirao and H. Ohara, *Polym. Rev.*, 2011, **51**, 1–22.

70 D. Bykowski, A. Grala and P. Sobota, *Tetrahedron Lett.*, 2014, **55**, 5286–5289.